

Giant thermoelectric effect in Al₂O₃ magnetic tunnel junctions

Weiwei Lin (林维维)[†], Michel Hehn, Laurent Chaput, Béatrice Negulescu[‡], Stéphane Andrieu, François Montaigne and Stéphane Mangin^{*}

Thermoelectric effects in magnetic nanostructures and the so-called spin caloritronics are attracting much interest.¹⁻¹¹ Indeed it provides a new way to control and manipulate spin currents which are key elements of spin-based electronics.^{12,13} Here we report on giant magnetothermoelectric effect in Al₂O₃ magnetic tunnel junctions. The thermovoltage in this geometry can reach 1 mV. Moreover a magneto-thermovoltage effect could be measured with ratio similar to the tunnel magnetoresistance ratio. The Seebeck coefficient can then be tuned by changing the relative magnetization orientation of the two magnetic layers in the tunnel junction. Therefore our experiments extend the range of spintronic devices application to thermoelectricity and provide a crucial piece of information for understanding the physics of thermal spin transport.

Thermoelectricity has been known since 1821 with T.J. Seebeck. On one hand, the relation between the thermal and the electrical transport is an essential topic for both fundamental physics and for the future of energy-saving technologies.^{14,15} On the other hand the discovery of the giant magnetoresistance effect (GMR) and the tunnel magnetoresistance effect (TMR) enhanced the interest of the community for spin-dependent conductivity and gave rise to spintronics and multiple applications.^{12,13} Its interplay with thermal conductivity was introduced to describe the conventional Seebeck effect in ferromagnetic metals.^{1-9,16-20} The magnetothermoelectric effect has then been studied in magnetic systems such as magnetic multilayers and spin valves.¹⁶⁻²⁰ Moreover the thermoelectric effect has also been observed in non magnetic tunneling devices such as superconductor-insulator-normal metal (or superconductor) tunnel junctions.^{21,22} Recently, thermal spin tunnelling effect from ferromagnet to silicon has been reported.²³ Concerning magnetic tunnel junction (MTJ), there were theoretical works²⁴⁻²⁶ showing magnetothermopower, however recent experimental studies in MgO MTJs^{27,28} showed the magnetic thermovoltage as weak as a few microvolts and are still under argument. In this letter, we present an experimental discovery of giant thermoelectric

effect in Al₂O₃ MTJs. The observed mV thermovoltage has promising application for the novel magnetic thermoelectric devices.

The studied MTJ consists of a bottom reference layer Ta(5 nm)/PtMn(25 nm)/Co₉₀Fe₁₀(2 nm)/Ru(0.8 nm)/Co₉₀Fe₁₀(3 nm) and a free layer Co₉₀Fe₁₀(2 nm)/Ni₈₀Fe₂₀(5 nm)/Ru(4.8 nm)/Au(10 nm) separated by a 2 nm thick amorphous Al₂O₃ barrier, as shown in Fig. 1a. To generate a temperature difference between the reference layer and the free layer, one electrode lead was heated using the laser beam from a laser diode with a wavelength of 780 nm and a tunable power from 0 to 125 mW. The temperature difference between both sides of the Al₂O₃ barrier is defined as ΔT whereas the voltage difference is ΔV . In the linear response approximation, the total electric current I in the presence of ΔV and ΔT can be written as

$$I = G_V \Delta V + G_T \Delta T \quad (1)$$

where G_V is the electrical conductance, and G_T is the thermoelectric coefficient related to the charge current response to the heat flux.

The thermovoltage ΔV can be measured in an open-circuit geometry where $I = 0$, as shown in Fig. 1b. Considering equation (1) it leads to $\Delta V = - (G_T/G_V) \Delta T = - S \Delta T$, where $S = G_T/G_V$ is the thermopower (TP) or Seebeck coefficient. ΔV was measured with a nanovoltmeter at room temperature (RT) with a magnetic field H applied along the in-plane easy axis. The thermotunnel current was measured by a source-meter connecting the MTJ without applied voltage, i.e. a closed-circuit, as shown in Fig. 1c. In the closed-circuit geometry, $\Delta V = 0$ and thus from equation (1), $I = G_T \Delta T$. With those two geometries the influence of magnetization orientations on both spin-dependent electrical conductivity and thermoelectric effect could be studied.

Figure 2a shows a minor loop of the tunnel resistance R as a function of the in-plane applied field H for an Al₂O₃ based MTJ. The MTJ has a low resistance $R_P = 15.9$ k Ω for the parallel (P) magnetizations alignment, and a high resistance $R_{AP} = 22.3$ k Ω for the antiparallel (AP) magnetizations alignment, showing a TMR ratio $(R_{AP} - R_P)/R_P = 40\%$.

Then, instead of injecting a current in the MTJ, as sketched in Fig. 1b, the voltage across the MTJ is measured in open-circuit geometry. The top lead is heated by the laser in order to generate a temperature

Institut Jean Lamour, Nancy-Université, Vandoeuvre-lès-Nancy 54506, France.[†]Present address: Institut d'Electronique Fondamentale, Université Paris-Sud, Orsay 91405, France; [‡]Present address: Laboratoire d'Electrodynamique des Matériaux Avancés, CNRS-CEA, Tours 37200, France; *e-mail: stephane.mangin@ijl.nancy-universite.fr.

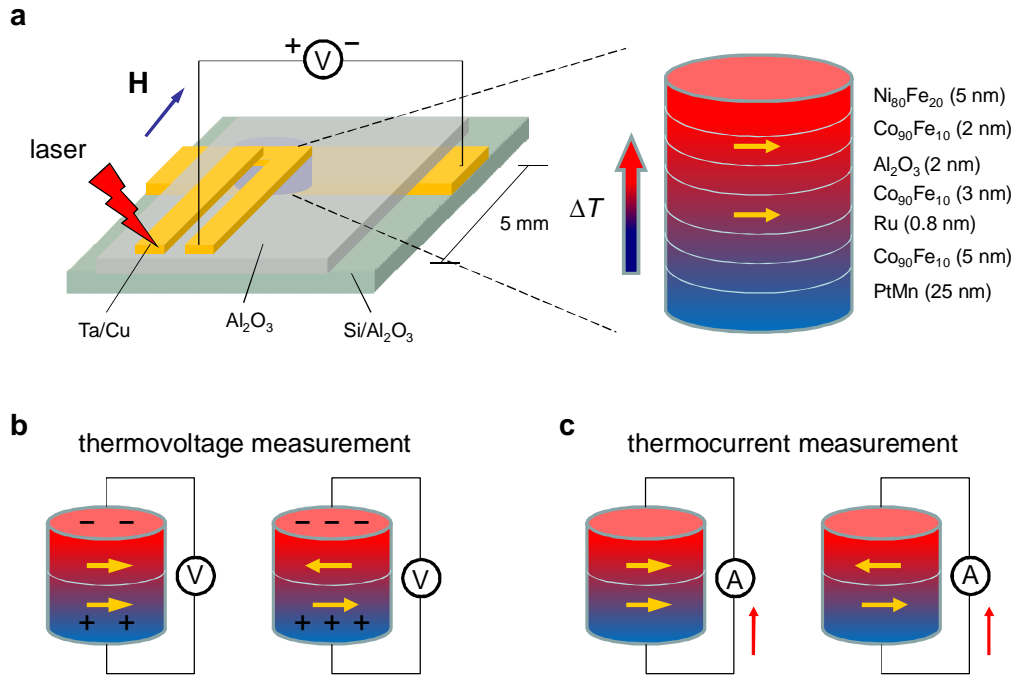


Figure 1 Schematic of the experiment. **a**, The studied MTJ consists of a bottom reference layer Ta(5 nm)/PtMn(25 nm)/Co₉₀Fe₁₀(2 nm)/Ru(0.8 nm)/Co₉₀Fe₁₀(3 nm) and a free layer Co₉₀Fe₁₀(2 nm)/Ni₈₀Fe₂₀(5 nm)/Ru(4.8 nm)/Au(10 nm) separated by an Al₂O₃ barrier. To generate a temperature difference between both sides of the Al₂O₃ barrier, one electrode lead was heated using the laser beam from a laser diode with the wavelength of 780 nm and the maximum power of 125 mW. The open-circuit voltage was measured by the nanovoltmeter at room temperature (RT) with an applied magnetic field H up to 3 kOe along the in-plane easy axis. **b**, In the presence of the temperature difference ΔT in the MTJ, the generated thermovoltage ΔV depends on the relative magnetization alignment of the two ferromagnetic layers. **c**, The thermotunnel current I was measured by the system sourcemeter connecting the MTJ in a closed-circuit without applied voltage.

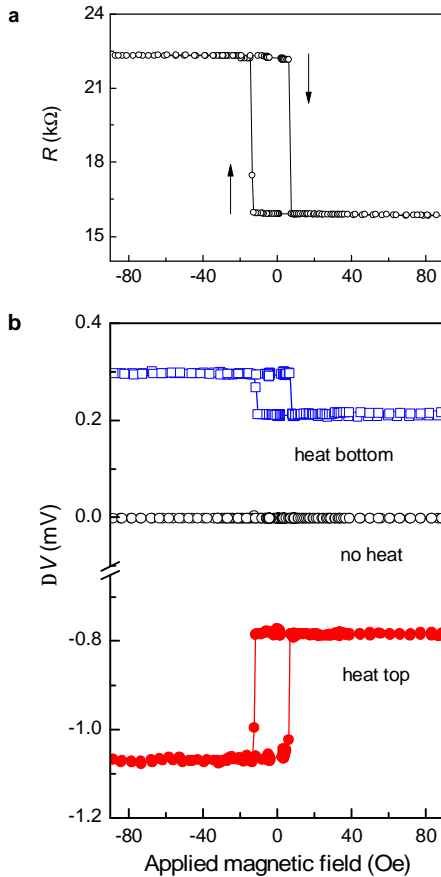


Figure 2 Magnetic field dependence of the tunnel resistance and the thermovoltage in a MTJ. **a**, The tunnel resistance R minor loop of an Al₂O₃ MTJ with the diameter of 80 μm as a function of H at RT, measured with a 0.1 μA current. The MTJ has a low resistance $R_P = 15.9$ k Ω for the parallel (P) magnetization alignment, and a high resistance $R_{AP} = 22.3$ k Ω for the antiparallel (AP) alignment, showing the TMR ratio $(R_{AP} - R_P)/R_P = 40\%$. **b**, The thermovoltage vs. applied field (V - H) minor loops. Instead of applying a current in the MTJ, the voltage across the MTJ is measured in open-circuit geometry with a laser heating the electrodes. As the laser heats the top lead, the temperature of the free layer is higher than that of the reference one, i.e. $\Delta T > 0$, yielding a negative thermovoltage ΔV , whereas a positive ΔV is observed in the case of the laser heating the bottom lead, i.e. $\Delta T < 0$. It is noted that the open-circuit voltage is zero in the incertitude of measurements in the absence of the laser heating. With sweeping the applied field, ΔV shows similar behavior with R . The amplitude of the thermovoltage for the AP alignment, ΔV_{AP} , is larger than that for the P one, ΔV_P . In our case, the ΔV_{AP} can be up to -1.07 mV as heating the top lead with the 125 mW laser power, while the ΔV_{AP} is about 310 μV as heating the bottom lead with the same laser power. The tunnel thermopower S can be estimated in the order of 1 mV K⁻¹. The tunnel magnetothermovoltage ratio defined as $(V_{AP} - V_P)/V_P$ is around 40%, which is similar with the TMR ratio of the MTJ. The result indicates that the thermovoltage ΔV is proportional to R in the MTJ.

difference between the free layer and the reference layer spaced by the Al_2O_3 barrier. With the top lead heated, the temperature difference is defined as positive $\Delta T > 0$. As shown in Fig. 2b a negative thermovoltage ΔV is detected in this geometry. While sweeping the in-plane applied field, a sudden ΔV jump is observed as the free layer magnetization switches and the magnetization configuration changes from P to AP. In fact the ΔV vs H hysteresis loop mimics the R vs H loop. Two thermovoltage levels are clearly defined corresponding to the two magnetization alignments (P and AP). The amplitude of the thermovoltage for the AP alignment, ΔV_{AP} , is found to be larger than that for the P one, ΔV_{P} . In our case, the ΔV_{AP} can reach up to -1.07 mV while heating the top lead with a 125 mW laser power. The ΔV_{AP} is about 310 μV when heating the bottom lead with the same laser power (see Fig. 2b). This difference can be understood since different material, thickness and size for the top and bottom leads result in different heat conductivity and dissipation. In the case where the laser heats the bottom lead, i.e. $\Delta T < 0$ then a positive thermovoltage is measured as shown in Fig. 2b and an inverse thermovoltage ΔV hysteresis loop is observed. Note that if the laser is turned off or shines the substrate instead of the leads, the thermovoltage drops to zero and no influence of the applied field is observed.

In the both cases of heating the top lead and the bottom one, the tunnel magnetothermoelectric ratio defined as $(\Delta V_{\text{AP}} - \Delta V_{\text{P}}) / \Delta V_{\text{P}}$ is around 40%, which is similar with the TMR ratio. This behavior suggests that the observed thermoelectric effect mainly results from the thermal spin-dependent tunneling between both sides of the Al_2O_3 barrier.

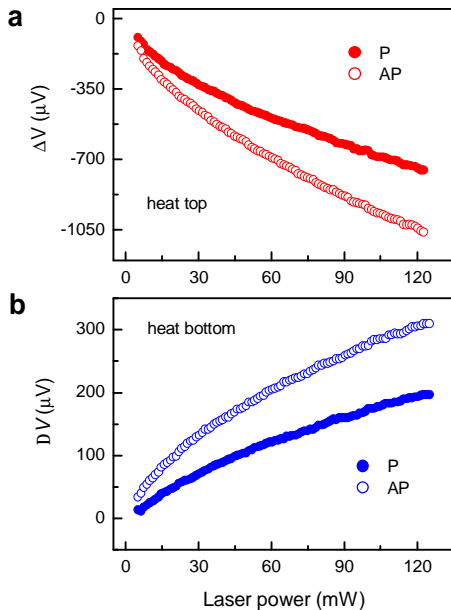


Figure 3 Laser power dependence of the magnetic thermovoltage in the MTJ. The thermovoltage ΔV_{P} and ΔV_{AP} as a function of the laser power P in the cases of heating the top lead (a) and the bottom (b). It is found that ΔV_{P} and ΔV_{AP} are proportional to $P^{1/2}$.

Figure 3 shows the thermovoltage ΔV_{P} and ΔV_{AP} as a function of the laser power P in the cases of heating the top lead (Fig. 3a) and the bottom (Fig. 3b). One can see

that the amplitudes of both ΔV_{P} and ΔV_{AP} increase with the laser power. Fitting of the experimental data, it can be found that ΔV_{P} and ΔV_{AP} behave as $P^{1/2}$ in the both cases of heating the top lead and the bottom.

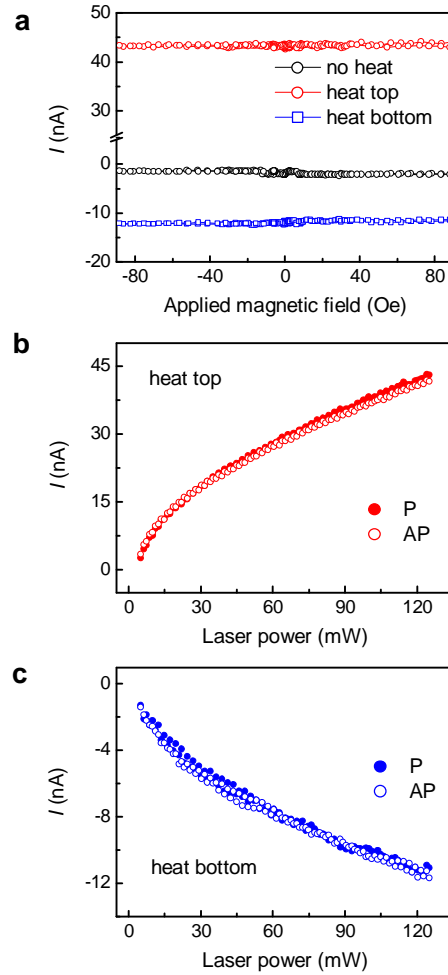


Figure 4 Magnetic field and laser power dependence of the thermotunnel current. a, Thermotunnel current vs. applied field (I - H) curves. I is independent on the magnetization alignments. b, c, The thermotunnel current I_{P} and I_{AP} as a function of the laser power P in the both cases of heating the top lead and the bottom. It is found that I_{P} and I_{AP} are proportional to $P^{1/2}$.

Figure 4a shows the measured thermotunnel current I as a function of H in a closed-circuit geometry as described above. Without the laser heating, the closed-circuit current is around zero. As heating the top lead by the 125 mW laser power, I is about 43 nA, and I is about -12 nA as heating the bottom lead by the same laser power. One can see that the thermotunnel current I is independent on the magnetization alignments. However similarly with the thermovoltage, the laser power dependence of the thermotunnel current is also proportional to $P^{1/2}$ in the both cases of heating the top lead and the bottom, as shown in Fig. 4b and Fig. 4c, which agrees with the thermotunnel current behaviors in the $\text{Al}/\text{Al}_2\text{O}_3/\text{PbBi}$ tunnel junction in Ref. 21. Considering the amplitude, the sign and the magnetic dependence of the measured signal, the possibility of an artifact coming from the known light-induced phenomena could be ruled out.

From the above results one can see that the thermovoltage ΔV is proportional to the MTJ resistivity whereas the thermotunnel current is independent on magnetizations relative orientations. From the experimental result, since the thermovoltage is given by $\Delta V = -(G_T/G_V) \Delta T = -S \Delta T$ whereas the thermocurrent is given by $I = G_T \Delta T$, assuming that for a fixed laser power ΔT is constant for the P and AP configuration, it leads to the conclusion that the coefficient G_T is independent on the magnetization alignments in the MTJ and consequently the thermopower S is proportional to resistivity. This means that in this MTJ sample we could define a tunnel thermopower S which depends strongly on the magnetization alignment of the two magnetic layers. To obtain the value of S , the temperature difference between both sides of the tunnel barrier is needed. Unfortunately it is hard to directly measure this difference. From measuring the temperature of the leads using either a thermocouple or the thermal variation of the leads resistance, we could conclude a temperature difference less than 1 K between the top and the bottom leads which could be much smaller between both sides of the tunnel barrier in the MTJ. The tunnel thermopower S can be estimated larger than 1 mV K⁻¹, which is larger than that in metals¹⁷⁻²⁰ and even larger than that in semiconductors^{14,15,29-31}. This means that giant thermopower can be obtained in a MTJ.

Such large magnetothermopower has neither been predicted nor been observed up to now. In the following we provide a simple model within the linear response theory that agrees with our finding. Note that this explanation does not exclude that this behaviour could result from a very peculiar inelastic scattering of the electrons with phonons or magnons, but in the absence of detailed experimental evidences of this type of process we will use a description based on elastic scattering only and find the particularities needed to explain the experimental data. In such a case it is possible to express the Onsager coefficient $L_{11} = G_V$ and $L_{12} = G_T$ as the moments of order 0 and 1 of the transport function $S^{(e)}$,

$$L_{11} = \int de S^{(e)} \left(-\frac{\partial f}{\partial e} \right) \quad L_{12} = \frac{1}{(-e)T} \int de S^{(e)} (e-m) \left(-\frac{\partial f}{\partial e} \right) \quad (2)$$

f is the Fermi-Dirac distribution function, and $(-e)$ the electron charge. The function $S^{(e)}$ has the physical meaning of an energy dependent conductivity for the electrons. The quantities L_{11} and L_{12} measure respectively the value and the slope of the function $S^{(e)}$, $k_B T$ around the Fermi level.

In the case of a P configuration, $S^{(e)}$ is given by

$$S_P(e) = \frac{2p}{\mathbf{h}} e^2 \left\{ |T_{\uparrow\uparrow}|^2 r_{\uparrow}^L r_{\uparrow}^R + |T_{\downarrow\downarrow}|^2 r_{\downarrow}^L r_{\downarrow}^R \right\} \quad (3)$$

whereas for an AP configuration,

$$S_{AP}(e) = \frac{2p}{\mathbf{h}} e^2 \left\{ |T_{\uparrow\downarrow}|^2 r_{\uparrow}^L r_{\downarrow}^R + |T_{\downarrow\uparrow}|^2 r_{\downarrow}^L r_{\uparrow}^R \right\} \quad (4)$$

$r_{\uparrow}^{L,R}$ and $r_{\downarrow}^{L,R}$ are the spin-up and spin-down density of states (DOS) in the left (L) and right (R) leads. $|T_{ss'}|^2$ are the tunneling functions. From $S = G_T/G_V = L_{12}/L_{11}$ it is clear that the thermopower will be proportional to the resistivity $1/L_{11}$, if L_{12} is independent of the magnetization orientation, as found in our experiment. In view of

equation (2) this requires the slope of the transport function, averaged $k_B T$ around the Fermi level, to be the same in the P and AP configuration. Notice that this does not preclude at all for the values of S_P and S_{AP} to be different and therefore allow observing a TMR. Neglecting the energy dependence of the tunneling functions, the slopes of $r_{\uparrow}^L r_{\uparrow}^R + r_{\downarrow}^L r_{\downarrow}^R$ and $r_{\uparrow}^L r_{\downarrow}^R + r_{\downarrow}^L r_{\uparrow}^R$ should then approximately be the same. Our experimental results would be consistent with DOS written as $r_{\uparrow} = r_{\uparrow}^{CoFe} + dr$ and $r_{\downarrow} = r_{\downarrow}^{CoFe} + dr$ where r_{\uparrow}^{CoFe} and r_{\downarrow}^{CoFe} are the DOS for an alloy of cobalt with iron, and dr a spin independent contribution. In such a case

$$S_P \propto r_{\uparrow}^{CoFe} r_{\uparrow}^{CoFe} + r_{\downarrow}^{CoFe} r_{\downarrow}^{CoFe} + 2(r_{\uparrow}^{CoFe} + r_{\downarrow}^{CoFe}) dr + 2dr^2 \quad (5)$$

$$S_{AP} \propto r_{\uparrow}^{CoFe} r_{\downarrow}^{CoFe} + r_{\downarrow}^{CoFe} r_{\uparrow}^{CoFe} + 2(r_{\uparrow}^{CoFe} + r_{\downarrow}^{CoFe}) dr + 2dr^2 \quad (6)$$

because spin up and spin-down DOS of bulk cobalt and iron have small slope at the Fermi level on the scale of $k_B T$, it is a good approximation to assume it is also true for their alloys, if no special atomic order is created, as it is in our compounds. The slopes of S_P and S_{AP} are then entirely given by the one of dr , and therefore independent of the P or AP configuration. This could explain why the thermocurrent of Fig. 4a is independent of the magnetization alignment. Moreover this would be consistent with the large value observed for the thermovoltage if dr is a resonance, for example originating from impurity states, since they are usually very narrow.

Then, we can obtain a coefficient G_T (L_{12}) almost independent of the magnetization orientation, whereas the tunnel thermopower S (L_{12}/L_{11}) will be inversely proportional to the electrical conductivity. This explains why the observed thermotunnel current is independent of the magnetization alignment and the tunnel thermopower is proportional to the tunnel resistance in our MTJ.

In summary, large thermoelectric effect was observed in the MTJ arising from the temperature difference between both sides of a 2 nm Al₂O₃ tunnel barrier. The magnetothermoelectric ratio for the P and AP magnetization configuration is similar with the TMR ratio, indicating that the tunnel thermopower is spin dependent and proportional to R in the MTJ. However the thermotunnel current is independent on the magnetization alignments. The thermopower can be estimated to be larger than 1 mV K⁻¹ in the MTJ which is larger than that in the metal and semiconductor, suggesting that MTJ can be used as a good thermospin device. The thermospin devices can work in an open-circuit without applying any current or voltage. On one hand, the large change in thermovoltage can be obtained in the presence of a temperature difference through controlling the relative magnetization alignment of the two ferromagnetic layers in the MTJ. On the other hand, the magnetothermoelectric can be used to detect the magnetization configuration even in the open-circuit geometry. The exact mechanism may still be discussed but we are proposing a description based on elastic scattering to explain qualitatively the experimental results.

This work extends the understanding of the spin-dependent thermal and electrical transport in

nanostructures, and has promising potential for the design and application of thermally driven magnetic tunnel junction.

Methods

MTJ preparation

The MTJ consists of a bottom reference layer Ta(5 nm)/PtMn(25 nm)/Co₉₀Fe₁₀(2 nm)/Ru(0.8 nm)/Co₉₀Fe₁₀(3 nm) and a free layer Co₉₀Fe₁₀(2 nm)/Ni₈₀Fe₂₀(5 nm)/Ru(4.8 nm)/Au(10 nm) separated by a 2 nm thick Al₂O₃ barrier. The films were deposited on the 400 nm Al₂O₃ covered Si wafers in a dc magnetron sputtering system at RT with a base pressure of 2×10^{-8} Torr and a deposition pressures of 2–3 mTorr. The Al₂O₃ barrier was obtained by reactive rf oxidation of a 2 nm Al layer at a power of 50 W. The films were annealed for 2 hours at the temperature of 265 °C and a 1.3 T magnetic field in a N₂ atmosphere oven, and then patterned to circular shape with the diameter varying from 40 to 100 μm using the photolithography and ion mill processes. The 200 nm Cu and 10 nm Ta were used as both the bottom and top leads. The MTJs were measured using a Keithley 2601A system sourcemeter. The TMR is around (40 ± 3)% and the resistance-area (RA) product is about (22 ± 6) MΩμm² at RT.

Magnetothermoelectric and thermotunnel current measurements

To generate a temperature difference between the reference layer and the free layer, the top lead or the bottom was heated using the laser beam from a laser diode with the wavelength of 780 nm and the maximum power of 125 mW. The laser spot on the lead is around 5 mm apart from the junction. The thermovoltage was measured by the nanovoltmeter in an open-circuit at RT with an applied magnetic field up to 3 kOe along the in-plane easy axis. The thermotunnel current was measured by the Keithley 2601A system sourcemeter connecting the MTJ in a closed-circuit without applied voltage.

The thermovoltage of MTJ was also checked by measuring the AC voltage using a lock-in SR830 with the same frequency of the AC laser power. The AC measurement shows the similar behavior with the DC measurement.

We measured the temperature difference in between the bottom and top leads using thermocouples. For a laser power of 125 mW, the temperature of the leads are 319±2 K, and the temperature difference between the top lead and the bottom one is 300±250 mK. The temperature difference across the barrier is estimated to be in the order of 100 mK.

The Al₂O₃ MTJs with the diameters varying from 40 to 100 μm were measured and showed similar behavior. (See Supplementary Information)

References

- Uchida, K. *et al.* Observation of spin Seebeck effect. *Nature* **455**, 778–781 (2008).
- Dubi, Y. & Di Venta, M. Thermospin effects in a quantum dot connected to FM leads. *Phys. Rev. B* **79**, 081302(R) (2009).
- Hatami, M., Bauer, G. E. W., Zhang Q. & Kelly, P. J. Thermoelectric effects in magnetic nanostructures. *Phys. Rev. B* **79**, 174426 (2009).
- Wang, R. Q., Sheng, L., Shen, R., Wang, B. G. & Xing, D. Y. Thermoelectric effect in single-molecule-magnet junctions. *Phys. Rev. Lett.* **105**, 057202 (2010).
- Uchida, K. *et al.* Spin Seebeck insulator. *Nature Mater.* **9**, 894–897 (2010).
- Jaworski, C. M. *et al.* Observation of spin-Seebeck effect in ferromagnetic semiconductor. *Nature Mater.* **9**, 898–903 (2010).
- Johnson, M. Spin caloritronics & the thermomagnetolectric system. *Sol. Sta. Comm.* **150**, 543–547 (2010).
- Takezoe, Y., Hosono, K., Takeuchi, A. & Tatara, G., Theory of spin transport induced by a temperature gradient. *Phys. Rev. B* **82**, 094451 (2010).
- Scheibner, R. *et al.* Thermopower of a Kondo spin-correlated quantum dot. *Phys. Rev. Lett.* **95**, 176602 (2005).
- Serrano-Guisan, S., Domenicantonio, G. D., Abid, M., Abid, J. P., Hillenkamp, M., Gravier, L., Ansermet, J. P. & Felix, C. Enhanced magnetic field sensitivity of spin-dependent transport in cluster-assembled metallic nanostructures. *Nature Mater.* **5**, 730–734 (2006).
- Fullerton, E. E. & Mangin, S. Origin of magnetothermoelectric V in cluster-assembled metallic nanostructures. *Nature Mater.* **7**, 257 (2008).
- Chappert, C., Fert, A. & Nguyen Van Dau, F. Emergence of spin electronics in data storage. *Nature Mater.* **6**, 813–823 (2007).
- Fert, A. Origin, development & future of spintronics. *Rev. Mod. Phys.* **80**, 1517–1530 (2008).
- Cahill, D. G. *et al.* Nanoscale thermal transport. *J. Appl. Phys.* **93**, 793–818 (2003).
- Jeffrey Snyder, G. & Toberer, E. S. Complex thermoelectric materials. *Nature Mater.* **7**, 105–114 (2008).
- Johnson, M. & Silsbee, R. H. Thermodynamic analysis of interfacial transport & of the thermomagnetolectric system. *Phys. Rev. B* **35**, 4959–4972 (1987).
- Conover, M. J. *et al.* Magnetothermopower of Fe-Cr superlattices. *J. Magn. Magn. Magn.* **102**, L5–L8 (1991).
- Piroux, L. *et al.* Large magnetothermoelectric power in Co-Cu, Fe-Cu & Fe-Cr multilayers. *J. Magn. Magn. Magn.* **110**, L247–L253 (1992).
- Baily, S. A. *et al.* Magnetothermopower of Co-Cu multilayers with gradient perpendicular to planes. *J. Appl. Phys.* **87**, 4855–4857 (2000).
- Gravier, L. *et al.* Spin-dependent thermopower in Co-Cu multilayer nanowires. *J. Magn. Magn. Magn.* **271**, 153–158 (2004).
- Smith, A. D., Tinkham, M. & Skocpol, W. J. New thermoelectric effect in tunnel junctions. *Phys. Rev. B* **22**, 4346–4354 (1980).
- Giazotto, F. *et al.* Opportunities for mesoscopics in thermometry & refrigeration. *Rev. Mod. Phys.* **78**, 217–274 (2006).
- Le Breton, J., Sharma, S., Saito, H., Yuasa, S. & Jansen R. Thermal spin current from ferromagnet to silicon by Seebeck spin tunneling. *Nature* **475**, 82–85 (2011).
- Wang, Z. C., Su, G. & Gao, S. Spin-dependent thermal & electrical transport in spin-valve system. *Phys. Rev. B* **63**, 224419 (2000).
- McCann, E. & Fal'ko, V. I. Giant magnetothermopower of magnon-assisted transport in ferromagnetic tunnel junctions. *Phys. Rev. B* **66**, 134424 (2002).
- Czerner, M., Bachmann, M. & Heiliger, C. Spin caloritronics in magnetic tunnel junctions: Ab initio studies. *Phys. Rev. B* **83**, 132405 (2011).
- Liebner, N. *et al.* Tunneling magnetothermopower in magnetic tunnel junction nanopillars. eprint arXiv 1104.0537v1.
- Walter, M. *et al.* Seebeck effect in magnetic tunnel junctions. *Nature Mater.* (2011) doi:10.1038/nmat3076.
- Hochbaum, A. I. *et al.* Enhanced thermoelectric performance of rough silicon nanowires. *Nature* **451**, 163–167 (2008).
- Boukai, A. I. *et al.* Silicon nanowires as efficient thermoelectric materials. *Nature* **451**, 168–171 (2008).
- Pernstich, K. P., Rössner, B. & Batlogg, B. Field-effect-modulated Seebeck coefficient in organic semiconductors. *Nature Mater.* **7**, 321–325 (2008).

Acknowledgements

The authors thank French National Research Agency (ANR) PNANO and ISTRADE for support. W. L. and S. M. thank J. Z. Sun Eric E Fullerton and A.D. Kent for the fruitful discussion.

Author contributions

W.L. conceived and designed the experiments, and performed the measurements and analysis. S.M. supervised the experiment. B.N. prepared the MTJ samples in this paper. M.H. and S.A. prepared the additional MTJ films and F.M. patterned the additional MTJ samples. W.L. and S.M. gave physical explanations and L.C. contributed to theoretical model. M.H. and S.A. contributed to the helpful discussions. W.L., L.C. and S.M. wrote the paper.

Supplementary Information

Magnetothermoelectric effect in $\text{Co}_{90}\text{Fe}_{10}/\text{Al}_2\text{O}_3/\text{Co}_{90}\text{Fe}_{10}$ tunnel junctions

We studied the thermoelectric effect for tens of Al_2O_3 based magnetic tunnel junctions (MTJs). Several devices with the same stack but various sizes were measured.

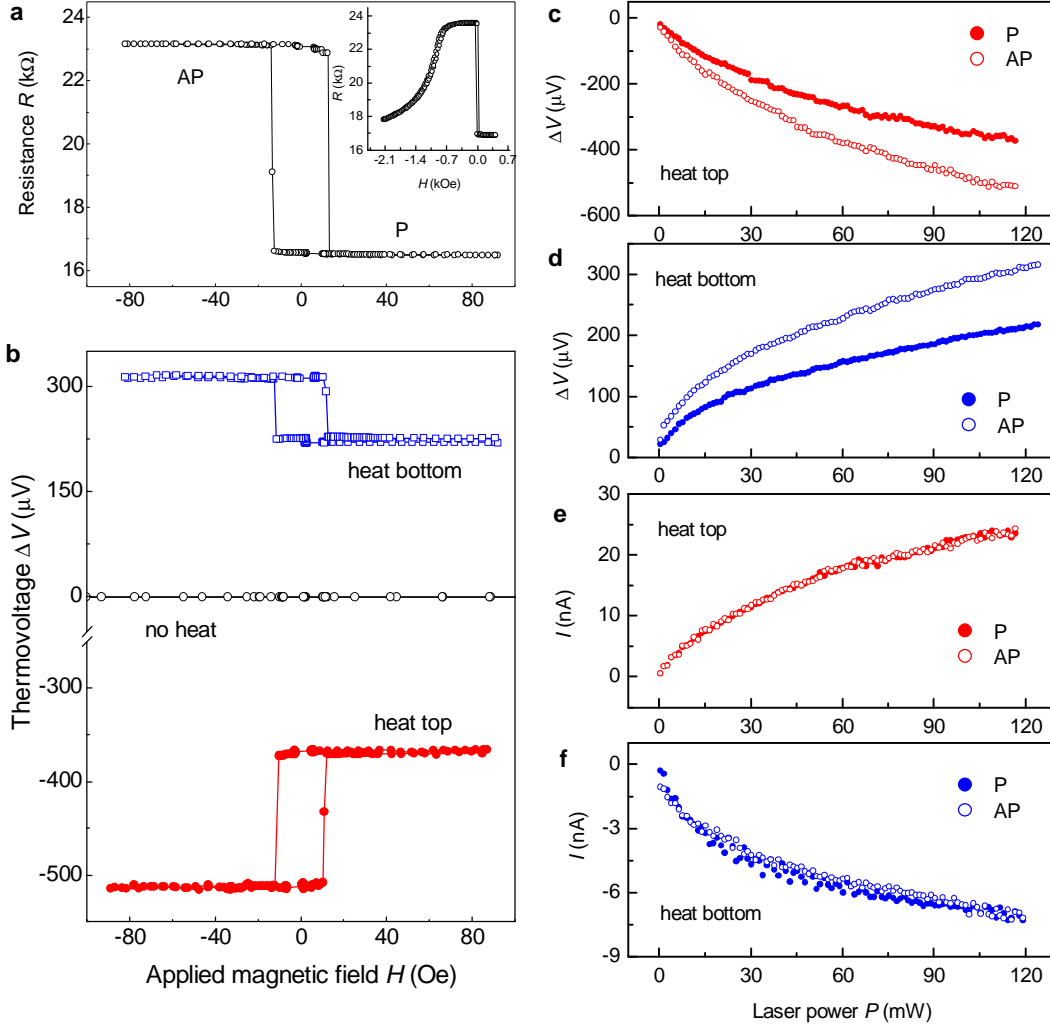


Figure S1 **a**, Magnetic minor loop of the tunnel resistance R in a Ta(5 nm)/PtMn(25 nm)/ $\text{Co}_{90}\text{Fe}_{10}$ (2 nm)/Ru(0.8 nm)/ $\text{Co}_{90}\text{Fe}_{10}$ (3 nm)/ Al_2O_3 (2 nm)/ $\text{Co}_{90}\text{Fe}_{10}$ (2 nm)/ $\text{Ni}_{80}\text{Fe}_{20}$ (5 nm)/Ru(4.8 nm)/Au(10 nm) MTJ with the diameter of 80 μm . The inset is the magnetic major loop of R . **b**, Magnetic loops of the thermovoltage ΔV in the MTJ. The red curve shows the case that the top lead is heated by the 125 mW laser, and the blue one indicates the case that the bottom lead is heated with the same laser power. **c,d**, Laser power P dependences of the thermovoltages ΔV_P and ΔV_{AP} in the cases of heating the top lead and the bottom, respectively. **e,f**, Laser power dependences of the thermotunnel currents I_P and I_{AP} in the cases of heating the top lead and the bottom, respectively.

Figure S1 shows the minor loops of the tunnel resistance and the thermovoltage as a function of the applied magnetic field in a Ta(5 nm)/PtMn(25 nm)/ $\text{Co}_{90}\text{Fe}_{10}$ (2 nm)/Ru(0.8 nm)/ $\text{Co}_{90}\text{Fe}_{10}$ (3 nm)/ Al_2O_3 (2 nm)/ $\text{Co}_{90}\text{Fe}_{10}$ (2 nm)/ $\text{Ni}_{80}\text{Fe}_{20}$ (5 nm)/Ru(4.8 nm)/Au(10 nm) MTJ. This device has the same stack and same size as the one studied in the paper. It gives very similar results: The tunnel resistance for the parallel (P) magnetization configuration R_P is 16.5 k Ω , and the TMR ratio is 40.6%. As the top lead is heated by the 125 mW laser, the open-circuit thermovoltage for the antiparallel (AP) magnetization configuration ΔV_{AP} is $-514 \mu\text{V}$, and the tunnel magnetothermoelectric ratio is 40.2%. The ΔV_{AP} is 315 μV as heating the bottom lead by the 125 mW laser, and the magnetothermoelectric ratio is 40.0%. ΔV_P and ΔV_{AP} behave as $P^{1/2}$ in both cases of heating the top lead and the bottom. The tunnel thermocurrent measured in a closed-circuit is 23 nA as heating the top lead with 125

mW laser power and is -7 nA as heating the bottom lead, which is no visible difference for the P and AP configurations.

Note that for the different pieces of MTJs, the thermovoltage can be different as heating the sample with the same laser power. This is because the thermovoltage is strongly related to the temperature difference between both sides of 2 nm tunnel barrier which is very small and could be different for the different pieces for the same laser power. Also, since for each experiment the laser does not shine the same position of the leads, we can argue that the temperature difference between both sides of the 2 nm tunnel barrier varies from one experiment to the other and so does the thermovoltage.

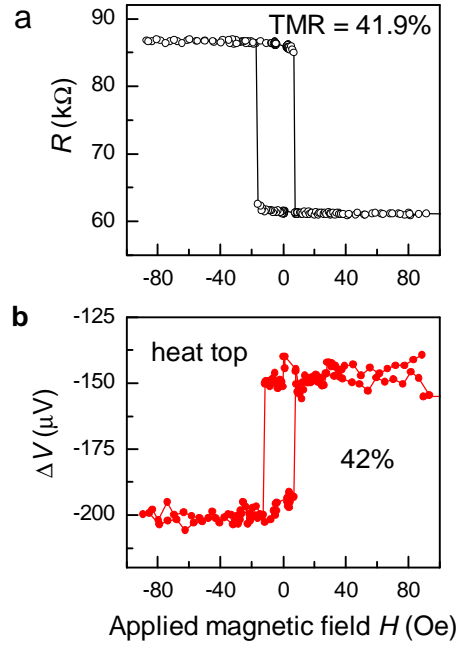


Figure S2 a, Magnetic minor loop of the tunnel resistance in a Ta(5 nm)/PtMn(25 nm)/Co₉₀Fe₁₀(2 nm)/Ru(0.8 nm)/Co₉₀Fe₁₀(3 nm)/Al₂O₃(2 nm)/Co₉₀Fe₁₀(2 nm)/Ni₈₀Fe₂₀(5 nm)/Ru(4.8 nm)/Au(10 nm) MTJ with the diameter of 40 μ m. **b**, Magnetic loop of the thermovoltage as heating the top lead with the 125 mW laser.

The Al₂O₃ MTJs with the diameters varying from 40 to 100 μ m were measured. Figure S2 shows the magnetic minor loops of the tunnel resistance and the thermovoltage in a Al₂O₃ MTJ with the diameter of 40 μ m. Similar behaviors are observed. The resistance R_P is 61.1 k Ω , and the TMR ratio is 41.9%. The thermovoltage ΔV_{AP} is -203 μ V as the top lead is heated by the 125 mW laser, and the magnetothermovoltage ratio is about 42% which is again very close to the TMR ratio.

These results confirm that the large amplitude of thermovoltage can be observed in these kinds of Al₂O₃ MTJs, that the magnetothermovoltage ratio is similar to the TMR ratio and that thermocurrent is constant for the P and AP configurations.